wjert, 2023, Vol. 9, Issue 10, 01-08. *Review Article* ISSN 2454-695X

World Journal of Engineering Research and Technology
WJERT
www.wjert.org SJIF Impact Factor: 5.924

NUMERICAL SIMULATION OF INTERNAL STEADY FLOW INSIDE A CYCLONE SEPARATOR

***Qi-Kai Gong, Bo Wang, Ji-Wei Shen, Ke-Xin Xie and Shi-Peng Li**

College of Mechanical Engineering, Quzhou University, Quzhou, 324000, China.

Article Received on 27/07/2023 **Article Revised on 17/08/2023** **Article Accepted on 07/09/2023**

***Corresponding Author**
Qi-Kai Gong
College of Mechanical Engineering, Quzhou University, Quzhou, 324000, China.

ABSTRACT

Cyclone separators are widely used in gas-liquid separation processes because of their high separation efficiency, small pressure drop and ease of maintenance. In this paper, by numerical simulation of a self-designed cyclone separator, we initially analyze the internal flow field of the cyclone separator under different inlet velocities when the medium is only air, and obtain the pressure cloud and velocity cloud in the longitudinal profile. It was shown that the overall internal pressure and internal velocity increased significantly with increasing inlet velocity.

KEYWORDS: Cyclone separators; Air; Internal flow field; Numerical simulation.

INTRODUCTION

A cyclone separator is a device used for the separation of gas-solid systems or liquid-solid systems. The working principle is to rely on the tangential introduction of airflow caused by the rotary motion, so that the solid particles or liquid droplets with large centrifugal force of inertia thrown to the outer wall to separate. In recent years, the industrial application of the soot purification equipment has received widespread attention, of which the most widely used is the cyclone separator; up to now, the cyclone separator has more than one hundred years of application history.[1] At present, it has been widely used in machinery, metallurgy, petroleum, coal, environmental protection, powder, electric power and many other fields; and in some industries, cyclone separators have become the most commonly used critical separation device.[2] Le Jianbo constructed a three-dimensional mathematical model of the gas-solid two-phase separation process based on the CFD method, and numerically simulated the velocity distribution, pressure distribution, and particle trajectory inside the ceramic particle cyclone using RSM and DPM models.[3] In order to study the short-circuit flow calculation method, Man Linxiang simulated and analyzed the internal flow field of the cyclone separator with the help of STAR-CCM+ software, and found that there exists an axial velocity zero point directly below the outer edge of the exhaust pipe, and the airflow between the point and the lower end of the exhaust pipe is closer to the real short-circuit flow, and a short-circuit flow calculation method for cyclone separator is proposed based on the axial velocity zero point.[4] Tang Shouqiang utilized CFD technology to numerically study the cyclone gas-phase flow field, gas-solid two-phase flow field, and particle trapping process using software such as Fluent.[5] Zhang Jian, Wang Yaying and others used the Reynolds stress model to numerically simulate the gas-phase flow field of the cyclone separator on the basis of which a double inlet spiral drag reduction device installed at the lower port of the cyclone exhaust mandrel was investigated.[6] Zhao Xinxue and Jin Youhai used numerical simulation to predict and analyze the wear problem of cyclone separators in industrial applications by using numerical simulation to predict and analyze the wear problem of their walls.[7] Qian Fuping and others used numerical simulation and based on the response surface method to obtain a prediction model of the natural cyclone length of the cyclone separator.[8] In this paper, the internal flow field of a self-designed cyclone separator under different inlet velocities is numerically simulated by numerical simulation techniques, expecting to get a preliminary grasp of the basic characteristics of the internal changes of the cyclone separator.

1 Numerical simulation methods

1.1 Calculation Model

Numerical simulation of a self-designed cyclone separator. The design parameters and main dimensions of the cyclone separator are shown in Figure 1 in meters.

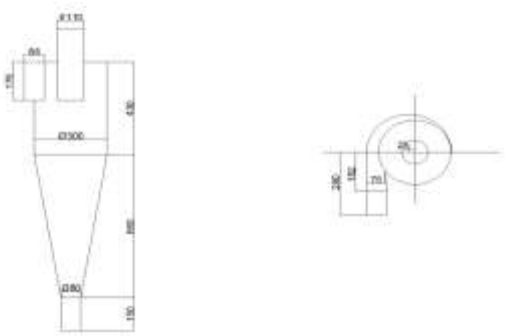

Figure 1: Model size.

1.2 Mesh Generation

ANSYS ICEM-CFD software was used for meshing as a pre-treatment process for numerical simulation. In order to obtain a high quality mesh, the model is divided into structured meshes in this paper. General generation steps for structured grids: 1. Import the model created in SOLIDWORKS; 2. Create Part; 3. Create the overall model Block and analyze the geometric model of the model to get the basic idea of chunking, and team Block for chunking; 4. According to the specific problem on the Block to carry out certain operations, such as stretching to get can express the structure of the geometric model of the block; 5. Establish mapping relationships; 6. Define the distribution of nodes on the Edge; 7. Generate the grid; 8. Check the quality of the grid; 9. Export the grid.

When creating the Part there are four main parts: entrance, upper exit, lower exit and wall. The total number of grids is around 300,000 and Figure 2 shows the gridding of the computational domain.

Figure 2: Computational Mesh.

1.3 Solution Control

Numerical calculations of three-dimensional, incompressible, non-stoichiometric, viscous fluids are performed using FLUENT 6.3, a commercial computational software based on the finite volume method. First set the gravitational acceleration to -9.81 m/s^2 in the Z direction, the inlet condition is that the inlet gas to the cyclone separator is selected from air at room temperature, the inlet is set to Velocity-inlet, inlet speeds of 1, 3 and 5 m/s respectively. In the Turbulence Model Settings dialog box, select the k-epsilon (2 eqn) model, selecting the submodel as RNG, activate Swirl Dominated Flow. Calculate the internal flow field when the inlet velocity is 1, 3 and 5 m/s, respectively. Velocity and pressure cloud maps were obtained on different cross sections and longitudinal profiles, respectively.

2 Results analysis

Figure 3 shows the pressure clouds in the tangential direction inside the cyclone separator for inlet velocities of 1, 3, and 5 m/s, respectively. From the three pressure clouds, it can be seen that the closer the pressure inside the cyclone separator is to the wall, the higher the pressure is; the pressure is highest at the inlet and lower at the upper and lower outlets; it is lowest at the center of the shaft. When the inlet speed is larger, the cyclone separator wall pressure has obvious growth, the pressure at the upper outlet and lower outlet has also become larger, while the pressure at the center of the shaft is sharply reduced, when the inlet speed is 5 m/s, the negative pressure value at the center of the shaft is extremely large, and can reach -140.76pa.

Figure 4 shows the velocity clouds in the tangential direction inside the cyclone separator for inlet velocities of 1, 3, and 5 m/s, respectively. From the three velocity clouds, it can be seen that the axial velocities in the cyclone are roughly symmetrically distributed along the center axis. Velocity is fast around the center axis, decreases the closer you get to the wall, and is fastest at the center of the axis. It can be seen that the gas velocity increases sharply here, so the pressure is minimum there. Velocity at both outlets becomes faster from the center to the wall. As the inlet velocity gets larger, there is a noticeable increase in velocity inside the cyclone separator.

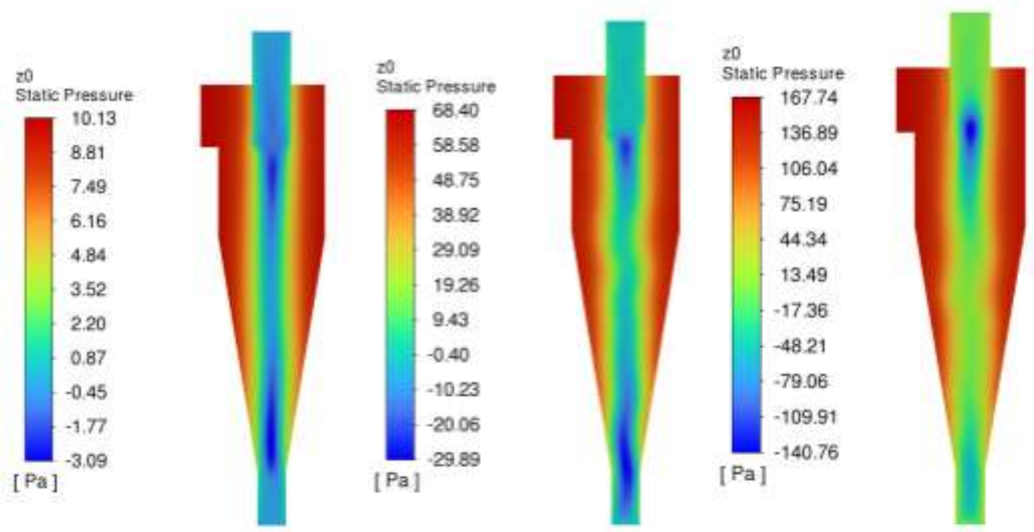

(a) 1m/s (b) 3m/s (c) 5m/s

Figure 3: Tangential Pressure Cloud.

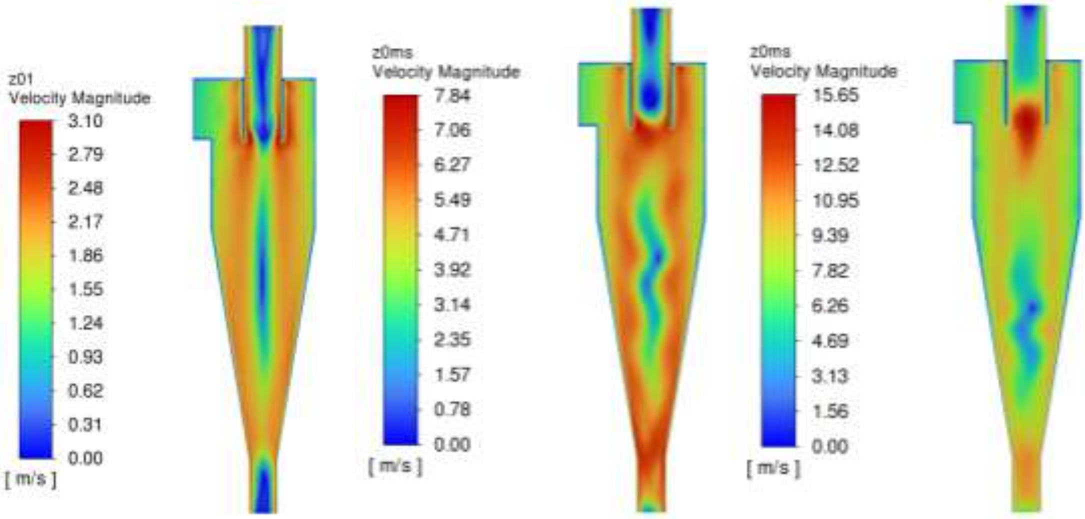

(a) 1m/s (b) 3m/s (c) 5m/s

Figure 4: Tangential Velocity Cloud.

The general characterization of the cyclone separator model was observed by taking cross sections of its characteristic surfaces at the inflection points. Figures 5, 6, and 7 show the pressure clouds of the cyclone separator at y=1160m, y=810m, and y=150m sections at inlet velocities of 1, 3, and 5 m/s, respectively. At different inlet velocities, the pressure inside the cyclone is characterized by a significant increase from the center axis to the periphery, and the pressure inside the separator decreases the closer you get to the lower outlet. The lowest pressure inside the cyclone is at the center shaft and increases significantly as the inlet velocity becomes larger.

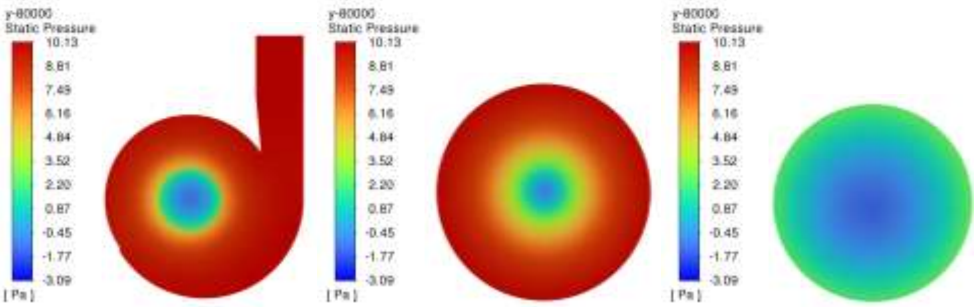

(a) y=1160m (b) y=810m (c) y=150m

Figure 5: Pressure clouds at different y sections at 1m/s.

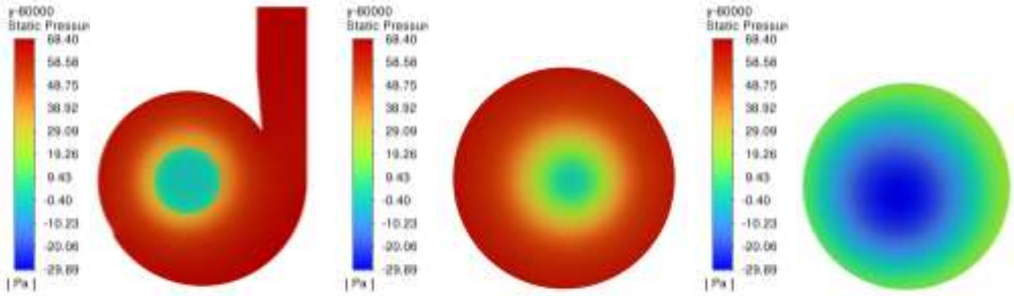

(a) y=1160m (b) y=810m (c) y=150m

Figure 6: Pressure clouds at different y sections at 3m/s.

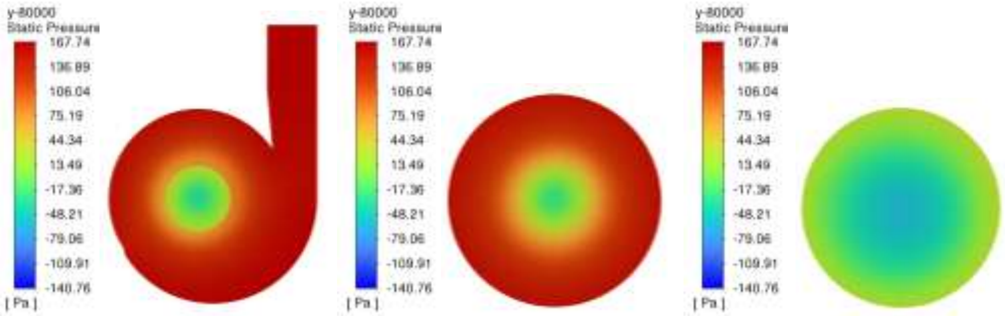

(a) y=1160m (b) y=810m (c) y=150m

Figure 7: Pressure clouds at different y sections at 5m/s.

Figures 8, 9, and 10 show the velocity clouds of the cyclone separator at y=1160m, y=810m, and y=150m cross sections at inlet velocities of 1, 3, and 5 m/s, respectively. From these plots, it can be observed that the faster cyclone velocities occur around the center shaft to the wall, and the pressures in the corresponding pressure clouds are relatively small. The fastest speeds in the separator are mainly distributed near the exit point. As the inlet velocity becomes larger, the velocities inside the cyclone separator all increase dramatically.

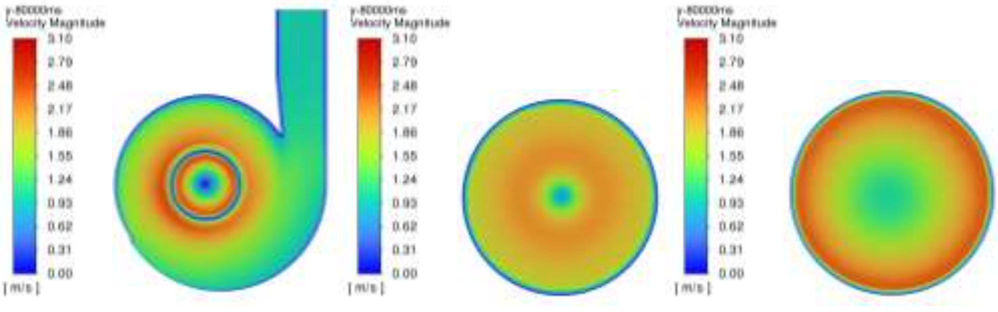

(a) y=1160m (b) y=810m (c) y=150m

Figure 8: Velocity clouds at different y sections at 1m/s.

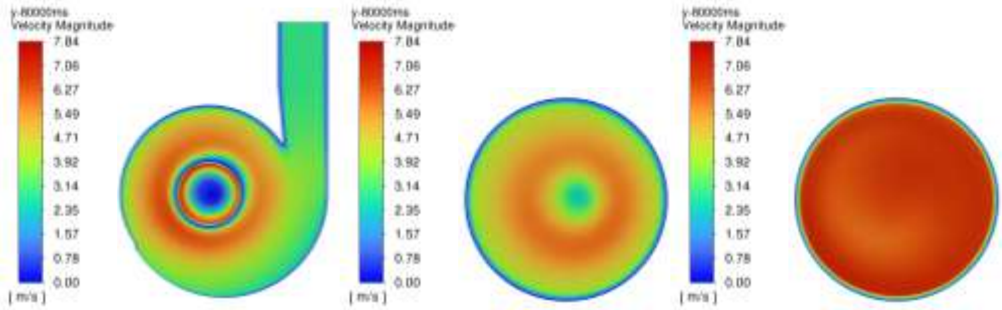

(a) y=1160m (b) y=810m (c) y=150m

Figure 9: Velocity clouds at different y sections at 3m/s.

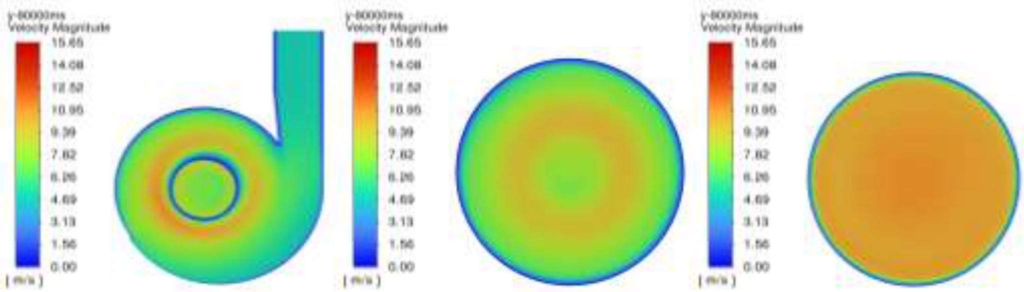

(a) y=1160m (b) y=810m (c) y=150m

Figure 10: Velocity clouds at different y sections at 5m/s

Figure 11 shows the velocity streamlines of the cyclone separator for inlet velocities of 1, 3 and 5 m/s, respectively. As can be observed at the upper and lower outlets of the three figures, the gas enters the cyclone through the inlet and leaves the separator while rotating. This means that the airflow exits not only with a certain axial velocity, but also with a certain tangential velocity, which makes it rotate and discharge, rather than simply linear.

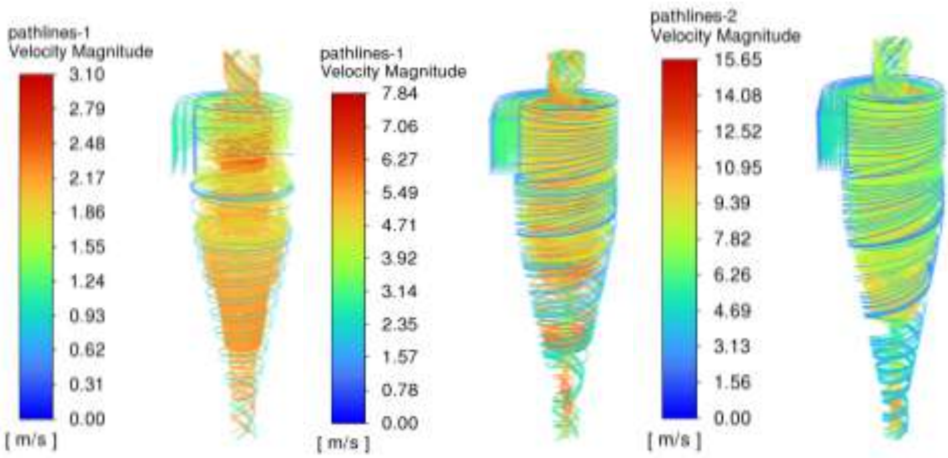

(a) 1m/s (b) 3m/s (c) 5m/s

Figure 11: Velocity Flow Chart.

CONCLUSION

1. As the inlet velocity increases, the overall internal pressure and internal velocity increase significantly.
2. The pressure inside the cyclone separator increases significantly from the center axial wall.
3. The airflow has both axial and tangential velocities as it exits.

The current study is only a preliminary computational model, and there are still a number of problems, such as whether the model selection is appropriate, whether the turbulence model selection is the most appropriate, and whether the solution control is the most economical and so on.

ACKNOWLEDGEMENTS

The work was supported by the national college students science and technology innovation project (No. 202211488028).

REFERENCE

1. PENG Wei-Ming, JI Zhong-Li. Cyclone Separator-Principle, Design and Engineering Application [M]. Beijing: Chemical Industry Press, 2004.
2. Liu Xiangdong, Yu Caiyuan. Commonly used industrial drying equipment and application [M]. Beijing: Chemical Industry Press, 2004.
3. LE Jianbo, PAN Yu'an, GAO Wenjie et al. Numerical simulation of the separation performance of ceramic particles and gas in cyclone separator based on CFD[J]. Liaoning Chemical Industry, 2023, 52(07): 974-978.
4. Man Linxiang. Analysis of CFD-based short-circuit flow calculation method for cyclone separator[J]. Digital Technology and Application, 2019, 37(09): 56-57.
5. Tang Shouqiang. Research on the influence of performance parameters of cyclone separator based on CFD [D]. Zibo: Shandong University of Technology, 2016.
6. ZHANG Jian, WANG Yaying, JIN Youhai. Study on drag reduction performance of cyclone separator based on CFD technology[J]. New Technology and New Process, 2007; (12): 46-49.
7. ZHAO Xinxue, JIN Youhai. Numerical prediction of cyclone wall wear based on CFD[J]. Petroleum Machinery, 2010, 38(12): 42-45.
8. Qian Fuping, Zhang Mingyao. Natural cyclone length of cyclone separator based on response surface method[J]. Journal of Southeast University, 2006; 36(2): 247-251.